Journal of the Serbian Chemical Society
JSCS-info@shd.org.rs • www.shd.org.rs/JSCS

J. Serb. Chem. Soc. *84* (5) 503–516 (2019)
JSCS–5203

UDC 546.62'28:620.17:620.193:
546.33'131–145
Original scientific paper

Mechanical properties and corrosion behaviour of Al–Si alloys for IC engine

JELENA ŠĆEPANOVIĆ[1], VANJA ASANOVIĆ[1], DRAGAN RADONJIĆ[1]*, DARKO VUKSANOVIĆ[1], SAFIJA HERENDA[2], FEHIM KORAĆ[2] and FARZET BIKIĆ[3]

[1]*University of Montenegro, Faculty of Metallurgy and Technology, Džordža Vašingtona bb, 81000 Podgorica, Montenegro,* [2]*University of Sarajevo, Faculty of Science, Department of Chemistry, Zmaja od Bosne 33–35, 71000 Sarajevo, Bosnia and Herzegovina and* [3]*University of Zenica, Faculty of Metallurgy and Technology, Travnicka cesta 1, 72000 Zenica, Bosnia and Herzegovina*

(Received 6 March, revised 29 March, accepted 11 April 2019)

Abstract: The paper describes the mechanical properties and the corrosion behaviour of three Al–Si alloys in 0.5 M NaCl solution. The alloys have exhibited similar values of hardness, but the highest tensile strength and the lowest elongation have shown the specimens of alloy with 11.38 % of silicon. Higher content of both copper and magnesium has contributed to better tensile strength and lower elongation of as-cast hypoeutectic alloys. The harmful effects of iron on mechanical properties of all alloys have been reduced to some extent by nickel and cobalt addition. The differences in the values of the open circuit potential of the examined alloys were insignificant. The thickness of the protective oxide layer has increased over time, and the layer has become very compact. Slight differences in the values of the corrosion potential of the alloys were determined, whereas the lowest value of the corrosion current was indicated for the hypereutectic alloy. The presence of intermetallic phases in the alloys has shown that the oxide film was not consistent. The severe pits have not been found at the surface of the corroded samples. Based on the obtained results, the examined alloys may be used for the manufacturing of the internal combustion engine parts.

Keywords: microstructure; Fe-based phase; Tafel curves.

INTRODUCTION

Aluminium and its alloys have, for an extended period of time, been of significant importance for everyday life due to an attractive combination of lightweight, high strength, and corrosion resistance.[1] Various registered compositions of aluminium casting alloys, possessing the properties consistent with specified requirements, as well as routine casting of aluminium parts are some of the advantages of designing those alloys, compared to other materials.[2] Aluminium castings con-

* Corresponding author. E-mail: draganra@ucg.ac.me
https://doi.org/10.2298/JSC190306030S

tinuously substitute the cast iron for engine blocks even for diesel vehicles.[3] The engine blocks, cylinder heads, and wheels are produced from hypoeutectic alloys.[4] The eutectic Al–Si alloys are used for large and thin-walled castings[4] while the hypereutectic Al–Si alloys are effectively applied for manufacturing of liner-less engine blocks, cylinder liners, cylinder heads, pistons and pumps.[5,6] The distribution of silicon particles in α-Al grains has a significant impact on the mechanical properties of Al–Si alloys.[7] Therefore, the control of the silicon phase structure influences the commercial application of these castings.[8] The nucleation and solidification cooling rate control the size of the primary silicon phase in hypereutectic Al–Si alloys, while the modification governs the size and morphology of eutectic silicon in hypoeutectic and eutectic Al-Si alloys.[9] The modification is based on the addition of a small amount of sodium, strontium, calcium, and antimony to hypoeutectic or eutectic Al–Si alloy.[8,10] The usual nucleation of silicon platelets is inhibited by chemical modifiers and eutectic aluminium grains initially formed, among which silicon is forced to grow,[9] acquiring a finer lamellar or fibrous eutectic morphology.[9,11]

The mechanical properties of aged Al–Si alloys are strongly affected by the addition of magnesium.[12] Copper is added for the strengthening effects in Al–Si alloys as well as the improvement of castability and machinability.[2] The addition of nickel could improve their strength and hardness at elevated temperatures.[13] On the other hand, the mechanical properties of Al–Si base alloys could be enhanced by refining the liquid materials.[14,15] The reinforcement of the microstructure of hypoeutectic alloys by increasing the concentration of silicon, manganese, and copper in Al–Si–Mg–(Cu) alloys could improve the durability of the automotive engine parts.[16] In order to improve the fluidity and castability of alloys intended for production of pistons and cylinder heads, beryllium is added in an amount of 0.01 to 0.05 %.[13] It was found that intermetallic compounds based on iron, which is a common impurity in those alloys, may reduce their mechanical properties,[17] but the most harmful effect is exhibited by the needle-shaped β-Al_5FeSi.[12] The sharp edges of needles or platelets of β-Al_5FeSi phase cause the high level of stress concentration and hence initiate the crack propagation.[18,19] In order to promote the formation of α-$Al_{15}Fe_3Si_2$ and prevent the appearance of β-Al_5FeSi in the microstructure of Al–Si alloys, they are alloyed with cobalt, molybdenum, chrome, nickel, and beryllium.[17]

The microstructure of Al–Si alloys defines not only mechanical properties but also corrosion resistance, to a great extent.[20] Therefore, the continuous examination of the dependence of corrosion behaviour on the microstructure of Al–Si base alloys is not surprising.[22–26] Despite the significant volume fraction of silicon in most of the Al–Si alloys, its influence of these alloys on the corrosion properties is minimal, because of the low corrosion current density that resulted from the high polarisation of silicon particles.[27] The local cells produced by iron and silicon pro-

mote the pitting attack on the surface of aluminium alloys in a conductive solution.[13] Although the mechanical properties of Al–Si–Mg casting alloys can be improved by precipitation of Mg_2Si phase, it is necessary to keep in mind that it will be accompanied by a decrease in their corrosion resistance.[28] The addition of copper to Al–Si alloys may change the corrosion resistance.[29] On the other hand, when combining the addition of magnesium and copper to achieve the appropriate properties of Al–Si casting alloys, the concentration of copper has to be between 1 and 3 %.[12] It was found that the susceptibility to intergranular corrosion of Al–Si––Mg(Cu) alloys is the result of micro galvanic coupling between CuSi and AlMgSiCu grain boundary precipitates in the adjacent depleted zones.[30] The addition of cobalt up to 0.5 % to Al–Si–Fe alloys could improve the corrosion resistance of as-cast and aged-hardened specimens.[31] The modification of Al–Si alloys with strontium results in a reduction of eutectic silicon particles and an increase in their density is accompanied by the provision of additional boundaries between α-Al and eutectic silicon phase.[32] Since those boundaries are susceptible to galvanic corrosion, the damaging effect of strontium on the corrosion resistance was found for the A356 alloy.[32] The corrosion behaviour of aluminium alloys depends on the localized aggressive environment containing halide anions which may cause breaking of the passivated surface of metal leading to the pitting.[22] Although different halide ions (Cl^-, Br^- and I^-) significantly accelerate stress--corrosion cracking, since chloride is present as both a natural constituent of marine environments and the contaminant of the environment, it is recognized as the most critical halide ion.[27]

This paper is concerned with the properties of as-cast Al–Si alloys aimed for the production of internal combustion engine parts. The alloys are designed with various amounts of silicon, magnesium, and copper as main alloying elements. Besides, the different content of iron, cobalt and nickel are defined in the examined alloys. The purpose of the study is to gain the insight into the influence of chemical composition on mechanical properties as well as the corrosion behaviour of the as-cast specimens in 0.5 M NaCl solution.

EXPERIMENTAL

Three alloys were prepared by melting several raw materials such as the AlSi10Mg master alloy, Al-base pre-alloys (Al, 33 % Cu, Al, 60 % Mn and Al, 75 % Fe) as well as the technically pure silicon, nickel and molybdenum. Beryllium was added within pre-alloy Al–5 % Be in the melts to improve fluidity and castability. The melting was carried out in a 20-kW electric resistance furnace using a graphite crucible, and the melting temperature was kept at 780±5 °C. For the fluxing of the melts, a TAL – 2 as a mixture of potassium chloride and sodium chloride with a small addition of cryolite was used. It was added in the amount of about 2 % of the melt quantity and reacted at a temperature of 690 °C. The melts were degassed with hexachloroethane tablets in the amount approximately equal to 0.25 % of each melt quantity. The Al-10 % Sr master alloy was added to the melts to modify the Al–Si eutectic. The melts were poured at 740±5 °C into the permanent grey cast iron moulds with a

thermal conductivity from 47 to 80 W/(m^2 K). The moulds were not preheated. After solidification, the castings were removed from the moulds and further cooled down to the room temperature. The chemical composition of the produced alloys is listed in Table I.

TABLE I. Chemical composition of examined alloys

Alloy	Content of the element, %										
	Si	Mg	Cu	Fe	Co	Ni	Be	Mo	Mn	Sr	Al
A	10.820	1.360	1.130	0.590	0.350	0.310	0.250	0.200	0.120	0.042	84.828
B	11.380	1.430	1.220	0.650	0.450	0.430	0.250	0.300	0.170	0.040	83.680
C	14.310	1.330	1.360	0.770	1.250	1.100	0.250	0.200	0.190	0.040	79.200

Tensile test specimens (4.0 mm gauge diameter and 45.0 mm gauge length) were machined from the as-cast alloys. The tensile strength and relative elongation of as-cast specimens were determined at room temperature using the machine 1195 Instron, whereas the hardness was determined as Brinell hardness HB 5/250/30 by means of a testing machine produced by Karl Frank Gmbh, type 38532. All data on tensile strength, hardness and elongation were determined as an average value of the three measurements at room temperature. The samples for microstructural examination cut from the cast bars were ground through the successive grades of silicon carbide abrasive papers followed by the water-based diamond and colloidal silica suspensions polishing. The etchant of 0.5 % HF was used for revealing the microstructure. As-cast microstructures were examined under an optical microscope and a scanning electron microscope – a JEOL JSM-6460 LV equipped with energy dispersive X-ray spectroscopy.

The as-cast specimens of the alloys have been cut into samples which have been ground with silicon carbide abrasive papers. The samples have been polished and cleaned in acetone. The electrochemical examinations were performed in a cell, containing a saturated calomel reference electrode (SCE), the platinum electrode as the counter electrode and Al–Si alloys as the working electrode, using the potentiostat/galvanostat 273 A and 5210 lock-in amplifier (Princeton Applied Research) supplied with SOFTCORR 352 II software. All potentials are referred to SCE. The corrosion behaviour of Al–Si alloys was examined at room temperature in 0.5 M NaCl solution by performing the open circuit potential measurements, the linear polarisation method, the potentiodynamic polarisation test, and cyclic voltammetry. The open circuit potential (OCP) of the alloy had been recorded for 60 min at ambient temperature. The Tafel extrapolation method was used for obtaining the potentiodynamic polarisation curves of the examined alloys over the range from –250 to 250 mV related to open circuit potential (OCP) at a scan rate 1mV s^{-1}. The corrosion kinetic parameters such as corrosion potential (E_{corr}), corrosion current density (j_{corr}), anodic Tafel slopes (β_a) as well as the cathodic Tafel slopes (β_c) are determined using the software installed in the instrument. The cyclic voltammetry was used to examine the diffusion processes between the electrolyte and the layer on the surface of the electrode. All cyclic voltammetry tests were performed in 0.5 M NaCl over the potential range from –0.1 to –0.7 V at a scan rate of 50 mV s^{-1}.

RESULTS AND DISCUSSION

The microstructure of as-cast specimens of the two hypoeutectic alloys A and B, as well as of the hypereutectic alloy C, are shown in Fig. 1. The dendrites of α-Al phase and modified eutectics were revealed in the alloys A and B (Fig. 1a and

b). The fine mixture of modified eutectic silicon and $Al_5Cu_2Mg_8Si_6$ phase was also observed. In the alloy C, the polyhedral or blocky primary silicon is distributed in a matrix containing dendrites of α-Al phase and eutectic silicon (Fig. 1c). Different intermetallic phases are revealed in all alloys. Intermetallic iron containing phase α-$Al_{15}(Fe,Mn)_3Si_2$ was observed with a polygonal morphology (Fig. 2). Besides, AlFeMoSi phase was discovered (Fig. 3) while Al_3Ni was occasionally observed in all alloys. Star-like crystals or regular polygonal crystals of (Fe, Mn, Cu, Mo, Co, Ni)Al_3 phase were discovered in all specimens (Fig. 1).

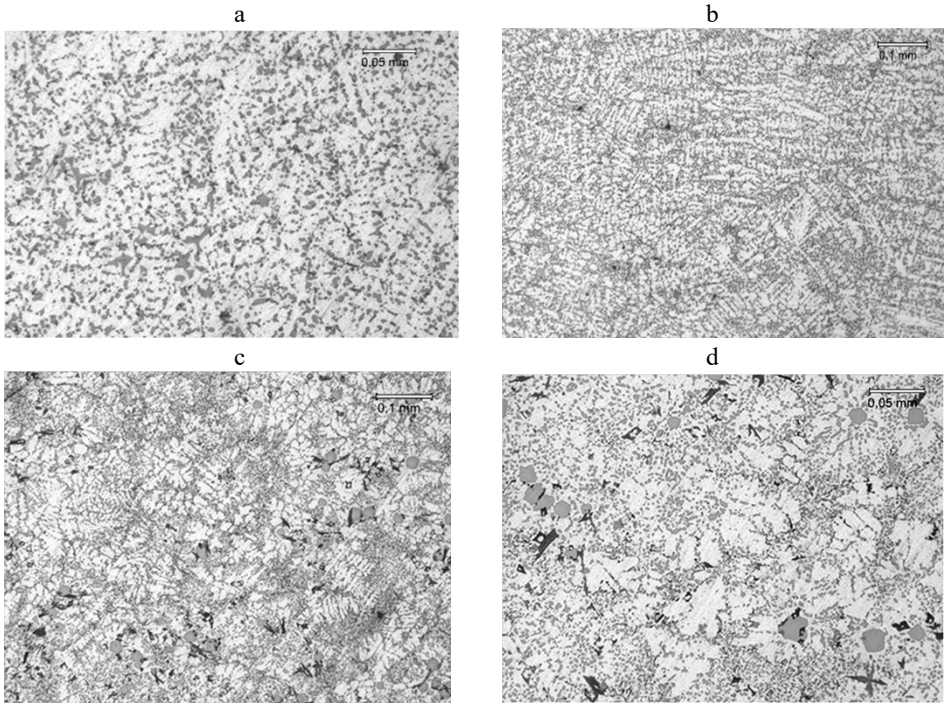

Fig. 1. Microstructure of as-cast specimens of alloys A (a), B (b) and alloy C (c and d).

The appearance of the mentioned phase despite the low iron content indicated the influence of copper amount on the microstructure as well as the alloy composition nonuniformity. The fine needles of β-$Al_5FeSi(Mn)$ phase confirmed the effect of crystallisation velocity. The microstructural examinations have shown the porosity (Fig. 1) which could be caused by air and gasses entrainment during the filling phase. However, Campbell and Tiriakioglu argued that besides the refinement of the eutectic silicon phase, the addition of strontium in Al–Si alloys could increase the tendency of the creation of casting porosity.[33] It is necessary to point out that the nature of the strontium action will depend on the preparation of melt and its quality before pouring, as well as the turbulence during the filling of the

mould.[33] Regarding our specimens, since the increase in the number and size of pores was not observed, it could be concluded that strontium had no harmful effect.

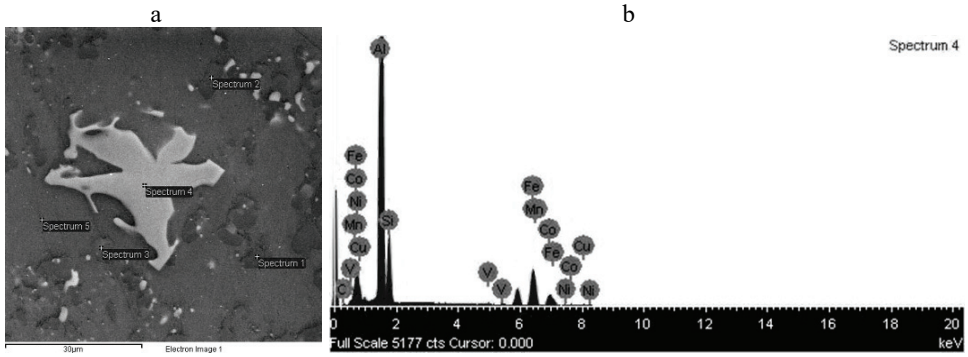

Fig. 2. a) Microstructure of as-cast specimen of alloy B and b) EDS analysis of the particles.

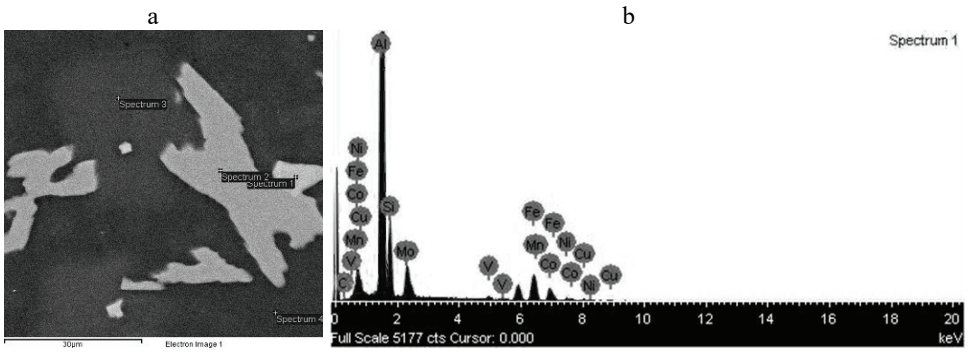

Fig. 3. a) Microstructure of as-cast specimen of alloy C and b) EDS analysis of the particles.

The mechanical properties of as-cast specimens shown in Table II are the result of the microstructural morphology as well as central porosity.

TABLE II. Mechanical properties of as-cast specimens

Alloy	Mechanical property		
	R_m / MPa	Hardness, HB	A / %
A	172.1	121.0	1.6
B	223.7	121.0	1.0
C	185.4	124.0	1.2

While similar values of hardness were identified for all alloys, the highest tensile strength and the lowest elongation were exhibited by as-cast specimens of alloy B containing 11.38 % of silicon. Although the low elongation in the range from 1.0 to 1.6 % was found for our alloys, it could be seen that such elongation is higher, when compared to the values recorded for Al–Si alloys (0.6 %) which are

not treated with strontium as explored by Farahany *et al.*[15] When comparing the hypoeutectic alloys A and B, it could be concluded that higher content of both copper and magnesium has contributed to better tensile strength and lower elongation. Although iron has formed intermetallic phases which have had damaging effects on the mechanical properties of all alloys, it is evident that nickel and cobalt mitigate that influence to some extent. The hypereutectic alloy C, containing the highest level of both nickel and cobalt, exhibited the tensile strength lower than hypoeutectic alloy B, due to the presence of the polyhedral or blocky primary silicon. Sui *et al*. have reported that the tensile strength of Al–Si–Cu–Ni–Mg alloys containing between 10.98 and 11.33 % of silicon was raised from 196 to 249 MPa, with the increase in the strontium amount from 0 to 0.02 %, whereas a decrease from 249 to 226 MPa was discovered with the further increase of the strontium content to 0.04 %.[34] Compared to mentioned alloys, it could be seen that our hypoeutectic alloy A has a lower tensile strength (172.1 MPa). The values of the tensile strength of the hypoeutectic alloy B (223.7 MPa) and Al–Si–Cu–Ni–Mg alloys containing 0.04 % of strontium are similar (226.02 MPa).[34] The low elongation determined for our alloys from 1.0 to 1.6 % is higher compared to the values recorded for Al-Si–Cu–Ni–Mg alloys regardless of the strontium content.[34]

The hypereutectic Al–18Si alloy in as-cast condition has shown a higher value of the tensile strength (205.7 MPa) compared to our alloy C (185 MPa), while exhibiting a lower elongation of 0.78 %.[35] On the other hand, regarding the hypereutectic Al–17.5 Si alloys with different content of iron and manganese studied by Bidmeshki *et al.*,[36] our alloy C, containing 14.31 % of silicon, has a higher value of hardness (124 HB) than the Al–17.5 Si alloy with 0.42 % of iron (about 116 HB). However, a further increase in the iron content has raised the hardness of Al–17.5 Si alloys.[36] Therefore, the alloys designated as 1.2FeMn (1.22 % of iron and 0.63 % of manganese) and 1.2FeMn (1.15 % of iron) exhibited a hardness similar to our alloy C(124 HB), but 1.8FeMn alloy (1.81 % of iron and 0.79 % of manganese) had a hardness of about 130 HB.[36]Al-Helal et al. reported that the tensile strength of Al-18Si alloy had increased by 14 % from 153.5 MPa for the conventionally cast, untreated samples to 175.1 MPa, for the castings which were treated with both phosphorus and strontium, but produced by a solid–liquid duplex casting process.[5] It can be seen that our hypereutectic alloy C containing 14.31 % of silicon, treated with strontium has exhibited a better tensile strength. The values of mechanical properties determined for the three Al-Si alloys are comparable with the level of guaranteed mechanical properties of standard Russian aluminium alloys.[12] Besides, a good agreement of those values with the mechanical properties determined for other Al-Si alloys suggests that our Al-Si alloys can find application as materials for the production of internal combustion engine parts.

The thermodynamical tendency of a material to the electrochemical oxidation in a corrosive medium could be evaluated on the basis of the open circuit potential.[37] The occurrence of oxidation, the formation of the passive layer or immunity may be accompanied by a variation of the open circuit potential which is stabilised around a stationary value after a period of immersion.[37] The open circuit potential changes of as-cast Al–Si alloys in a 0.5 M NaCl solution as a function of immersion time are shown in Fig. 4.

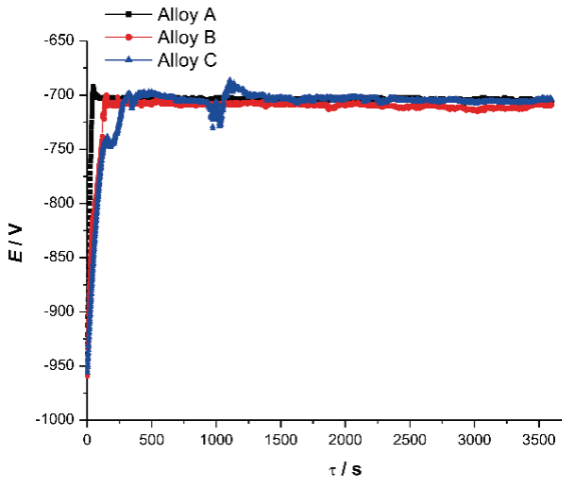

Fig. 4. Open circuit potential changes for the examined Al–Si alloys in 0.5 M NaCl solution.

The steady-state corrosion was established at the surface of the samples immersed in the electrolyte, and the current of anodic dissolution of metal and the cathodic reduction current were of the same value, but of the opposite direction. The differences in the values of open circuit potential of all alloys were not significant. Initially, the potential of the examined alloys was in the range from –939 to –959 mV, but the final values were similar (Table III). The steady-state value of open circuit potential was reached after 80 s for alloy A, while 140 and 280 s were necessary for alloy B and C, respectively. The shift of the potential of the alloys to a more positive values area indicates the occurrence of the passivation and the formation of an oxide layer at the surface of the alloy decreasing the corrosion rate.

TABLE III. Open circuit potential values of cast Al–Si alloys: initially and after 60 minutes of immersion in 0.5 M NaCl solution

Alloy	*E* / mV *vs.* SCE	
	Initial	Final
A	–939	–706
B	–959	–709
C	–956	–704

The thickness of the protective oxide layer had increased over time, and the layer became very compact. The barrier oxide film which is formed on the metal surface represents a product of the interaction of the metal and the oxidising agent. Following the theory of passive coating, the rate of chemical dissolution of the passive layer determines the corrosion rate of metal in a passive state.[38]

The linear polarisation method was applied to study the corrosion rate data. The potential (E) *vs.* current density (j_{corr}) was measured around ± 20 mV relative to the open circuit potential of the alloys. The obtained results (Fig. 5 and Table IV) show that the examined alloys are corrosive stable in 0.5 M NaCl solution. The corrosive rate of all alloys was slow.

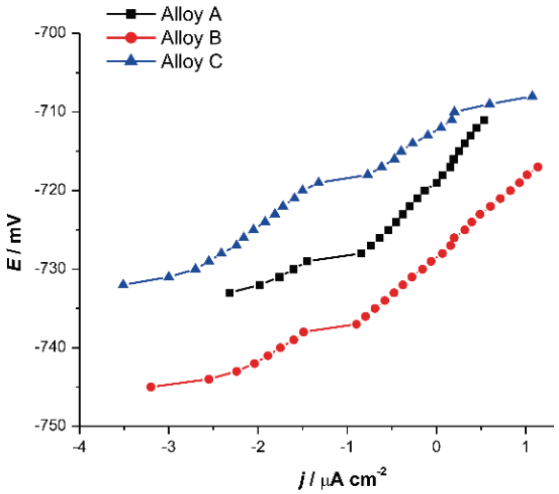

Fig. 5. Linear polarisation of cast Al–Si alloys.

TABLE IV. The results of linear polarisation method

Alloy	$E_{(I=0)}$ / mV	R_P / kΩ	j_{corr} / μA cm^{-2}
A	–712.5	6.093	3.564
B	–727.6	7.812	2.780
C	–718.2	9.516	2.282

The potentiodynamic polarisation curves of cast Al-Si alloys are shown in Fig. 6. The corrosion current density was recorded over the cathodic and anodic potential regions at a scan rate of 1 mV s^{-1}. The small change in the current density is observed within the cathodic and the anodic branches indicating the low corrosion rate of the cast Al–Si alloys in 0.5 M NaCl. The Tafel extrapolations of the corrosion current density (j_{corr}), the corrosion potential (E_{corr}) and the corrosion rate, as well as the values of anodic Tafel slopes (β_a) and cathodic Tafel slopes (β_c) are shown in Table V. The passive layer on the surface of the cast Al–Si alloys appeared at the corrosion potential which compared to –750 mV and

moved towards a more positive value. The anodic current slowly increased until the breakdown potential of about –675 mV was reached, but above it, the density of the current was rising rapidly, suggesting the breakdown of the passive layer due to the pitting corrosion.[39] The significant differences in the values of corrosion potential of the examined alloys were not observed, whereas the lowest value of corrosion current was determined for alloy C.

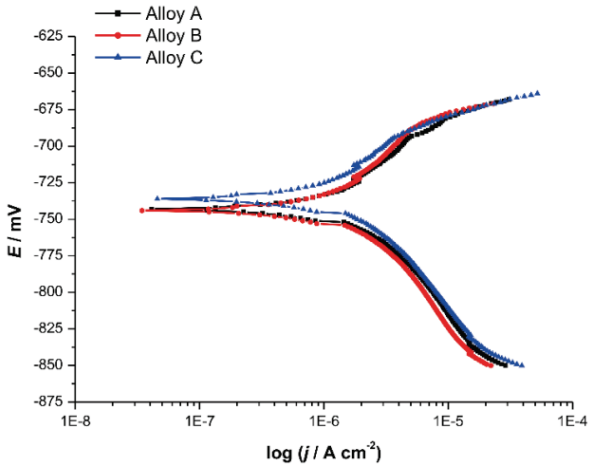

Fig. 6. Potentiodynamic polarisation curves of cast Al–Si alloys.

TABLE V. Electrochemical parameters calculated for cast Al–Si alloys in 0.5 M NaCl solution

Alloy	$E_{(I=0)}$ / mV	OCP, mV	β_c / mV dec^{-1}	β_a / mV dec^{-1}	j_{corr} / μA cm^{-2}
A	–743.0	–721.0	115.9	119.7	2.655
B	–744.0	–719.0	146.4	186.5	3.374
C	–735.9	–723.0	100.7	94.1	1.948

Kaiser *et al*. studied the corrosion behaviour of the commercially available aluminium alloys for the manufacturing of an engine block and piston in 0.1 M NaCl solution.[40] The potentiodynamic polarisation study has shown the corrosion potential (E_{corr}) as –764 mV for the engine block alloy and –622 mV for the piston alloy.[40] The values of the corrosion potential obtained for our alloys were from –735.9 to –744.0 mV, which indicated a shift to more positive values, compared to an engine block alloy, but more negative values concerning the piston alloy. Higher content of nickel (from 0.31 to 1.1 %) and lower concentration of iron (from 0.59 to 0.77 %) in our alloys could explain the observed difference in E_{corr} compared to the engine block alloy containing 0.083 % of nickel and 0.795 % of iron.[40] However, higher content of magnesium in our alloys (from 1.3 to 1.43 %) with regard to commercially available piston alloy containing 0.492 %,[40] could be the reason for the shift in the corrosion potential of about 114 or 122 mV to more negative values.

Cyclic voltammetry was used to study the influence of chlorides on the oxidation and reduction processes at the surface of cast Al–Si alloys. Fig. 7 shows the cyclic polarisation curves for the examined alloys in 0.5 M NaCl solution carried out in the range of potential between –1.0 and –0.4 V *vs*. SCE and the scan rate of 50 mV s^{-1}. The current density increase was associated with the formation of the oxide layer. After completely covering the surface with the oxide layer, the current density decreased indicating the onset of passivation. The values of the pitting potential (E_{pitt}) and repassivation potential (E_{repass}) obtained by cyclic voltammetry for the examined Al–Si alloys are similar, as shown in Table VI.

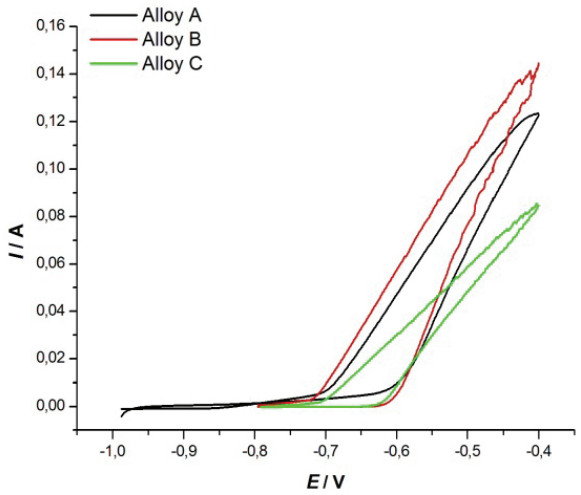

Fig. 7. Cyclic voltammograms for cast Al–Si alloys.

TABLE VI. The results of cyclic voltammetry

Alloy	E_{pitt} / V	E_{repass} / V
A	–0.60	–0.70
B	–0.61	–0.72
C	–0.63	–0.71

The applied methods have shown the similar corrosion behaviour of the three as-cast Al–Si alloys. The presence of intermetallic phases in the examined alloys has shown that the oxide film was not consistent. It is known that the difference in the corrosion potential among α-Al matrix and intermetallic phases can cause the formation of micro-galvanic cells.[41] Consequently, the alloying elements determine the overall corrosion behaviour of as-cast specimens. It is important to note that severe pits have not been found at the surface of the corroded samples. Therefore, in addition to the determined mechanical properties, the corrosion behaviour of the examined alloys in 0.5 M NaCl recommends those materials for manufacturing the internal combustion engine parts.

CONCLUSIONS

The three as-cast Al–Si alloys designed with various amounts of silicon, magnesium and copper as main alloying elements have exhibited similar values of hardness. However, the highest tensile strength and the lowest elongation have shown specimens of alloy hypoeutectic B containing 11.38 % of silicon. The hypereutectic alloy C containing the highest level of both nickel and cobalt exhibited tensile strength lower than alloy B due to the presence of the polyhedral or blocky primary silicon. The higher content of both copper and magnesium has contributed to better tensile strength and lower elongation of hypoeutectic alloys A and B. Nickel and cobalt have reduced the harmful effects of iron on the mechanical properties of all alloys to some extent. Beside the microstructural morphology, the central porosity had an impact on the mechanical properties of the examined alloys.

The applied methods discovered similar corrosion behaviour of the three as-cast Al–Si alloys. The steady-state value of the open circuit potential was reached after 80 s for alloy A (10.82 % Si), while 140 and 280 s were needed for alloy B (11.38 % Si) and alloy C (14.31 % Si), respectively. The corrosive rate of all alloys was slow. The occurrence of passivation and formation of the protective oxide layer at the surface was indicated by the shift in the potential of the alloys to a more positive value. The thickness of the protective oxide layer has increased over time, and the layer has become very compact. Slight differences in the values of the corrosion potential were determined for the examined alloys, whereas the lowest value of the corrosion current was indicated for the hypereutectic alloy C.

The presence of the intermetallic phases in the examined alloys has shown that the oxide film was not consistent. However, severe pits have not been found at the surface of the corroded samples. Therefore, in addition to the mechanical properties which are in reasonable accordance with the results obtained by various researchers for similar materials, the corrosion behaviour suggests that our Al–Si alloys can find application in the production of the internal combustion engine parts.

ИЗВОД

МЕХАНИЧКА СВОЈСТВА И КОРОЗИОНО ПОНАШАЊЕ Al–Si ЛЕГУРА ЗА МОТОРЕ СА УНУТРАШЊИМ САГОРЕВАЊЕМ

ЈЕЛЕНА ШЋЕПАНОВИЋ[1], ВАЊА АСАНОВИЋ[1], ДРАГАН РАДОЊИЋ[1], ДАРКО ВУКСАНОВИЋ[1], САФИЈА ХЕРЕНДА[2], ФЕХИМ КОРАЋ[2] и ФАЗРЕТ БИКИЋ[3]

[1]Универзитет Црне Горе, Металуршко–технолошки факултет, Цорца Вашингтона бб, 81000 Подгорица, Црна Гора, [2]Универзитет у Сарајеву, Природно-математички факултет, Одсјек за хемију, Змаја од Босне 33–35, 71000 Сарајево, Босна и Херцеговина и [3]Универзитет у Зеници, Металуршко–технолошки факултет, Травничка цеста 1, 72000 Зеница, Босна и Херцеговина

У овом раду су проучаване механичке особине и корозионо понашање три Al–Si легуре у 0.5 M NaCl раствору. Сличне вредности тврдоће испољиле су све легуре, али су највећу затезну чврстоћу и најмање издужење показали узорци од легуре са 11,38 %

силицијума. Већи садржај бакра и магнезијума допринео је бољој затезној чврстоћи и мањем издужењу ливених подеутектичких легура. Штетни ефекти гвожђа на механичке особине свих легура у извесној мери су ублажени додавањем никла и кобалта. За испитиване легуре нису утврђене значајне разлике вредности потенцијала отвореног кола. Дебљина заштитног оксидног слоја се повећавала са временом, и слој је постао веома компактан. Утврђене су мале разлике у вредностима корозионог потенцијала легура, док је најнижа вредност струје корозије назначена за надеутектичку легуру. Присуство интерметалних фаза у легурама показало је да оксидни филм није био конзистентан. Дубоке јамице нису пронађене на површини узорака након корозије. На основу добијених резултата, испитиване легуре се могу користити за израду делова мотора са унутрашњим сагоревањем.

(Примљено 6. марта, ревидирано 29. марта, прихваћено 11. априла 2019)

REFERENCES

1. J. G. Kaufman, *Introduction to aluminum alloys and tempers*, ASM International, Materials Park, OH, 2000, p. 1 (ISBN 978-0-87170-689-8)
2. J. G. Kaufman, E. L. Rooy, *Aluminum Alloy Castings: Properties, Processes, and Applications*, ASM International, Materials Park, OH, 2004, pp. 2, 13 (ISBN 0-87170-803-5)
3. J. Hirsch, *Trans. Nonferrous Met. Soc. China* **24** (2014) 1995 (https://doi.org/10.1016/S1003-6326(14)63305-7)
4. C. G. Shivaprasad, K. Aithal, S. Narendranath, V. Desai, P. G. Mukunda, *Int. J. Microstruct. Mater. Prop.* **10** (2015) 274 (https://doi.org/10.1504/IJMMP.2015.072921)
5. K. Al–Helal, I. C. Stone, Z. Fan, *Trans. Indian Inst. Met.* **65** (2012) 663 (https://doi.org/10.1007/s12666-012-0171-4)
6. A. Ahmed, M. S. Wahab, A. A. Raus, K. Kamarudin, Q. Bakhsh, D. Ali, *Indian J. Sci. Technol.* **9** (2016) 1 (https://doi.org/10.17485/ijst/2016/v9i36/102155)
7. B. D. Baliga, K. N. Mohandas, T. A. Kumar, *Int. J. Eng. Sci. Inn. Technol.* **4** (2015) 310 (http://www.ijesit.com/Volume%204/Issue%203/IJESIT201503_42.pdf)
8. G. K. Sigworth, *Int. J. Metalcast.* **2** (2008) 19 (https://doi.org/10.1007/BF03355425)
9. J. Jorstad, D. Apelian, *Int. J. Metalcast.* **3** (2009) 13 (https://doi.org/10.1007/BF03355450)
10. J. R. Davis, *Alloying: Understanding the Basics*, ASM International, Materials Park, OH, 2001, p. 392 (ISBN 978-0-87170-744-4)
11. F. C. Robles-Hernandez, J. M. H. Ramírez, R. Mackay, *Al-Si Alloys: Automotive, Aeronautical, and Aerospace Applications*, Springer, Cham, 2017, p. 187 (https://doi.org/10.1007/978-3-319-58380-8)
12. V. S. Zolotorevsky, N. A. Belov, M. V. Glazoff, *Casting Aluminum Alloys*, Elsevier, Oxford, 2007, pp. 328, 329, 496 (ISBN 978-0-08-045370-5)
13. J. E. Hatch, *Aluminum: Properties and Physical Metallurgy*, American Society for Metals, Metals Park, OH, 1984, pp. 224, 235, 279 (ISBB 0871701766)
14. X. Dong, Y. Zhang, J. Shouxun, *Mater. Sci. Eng., A* **700** (2017) 291 (https://doi.org/10.1016/j.msea.2017.06.005)
15. S. Farahany, A. Ourdjini, H. R. Bakhsheshi-Rad, *Trans. Nonferrous Met. Soc. China* **26** (2016) 28 (https://doi.org/10.1016/S1003-6326(16)64085-2)
16. C. Y. Jeong, *Mater. Trans., JIM* **54** (2013) 588 (https://doi.org/10.2320/matertrans.M2012285)
17. M. Rejaeian, M. Karamouz, M. Emamy, M. Hajizamani, *Trans. Nonferrous Met. Soc. China* **25** (2015) 3539 (https://doi.org/10.1016/S1003-6326(15)63951-6)
18. M. Karamouz, M. Azarbarmas, M. Emamy, M. Alipour, *Mater. Sci. Eng., A* **582** (2013) 409 (https://doi.org/10.1016/j.msea.2013.05.088)

19. J. O. Lima, C. R. Barbosa, I. A. B. Magno, J. M. Nascimento, A. S. Barros, M. C. Oliveira, F. A. Souza, O. L. Rocha, *Trans. Nonferrous Met. Soc. China* **28** (2018) 1073 (https://doi.org/10.1016/S1003-6326(18)64751-X)
20. W. R. Osório, P. R. Goulart, A. Garcia, *Mater. Lett.* **62** (2008) 365 (https://doi.org/10.1016/j.matlet.2007.05.051)
21. A. M. Cardinale, D. Macciò, G. Luciano, E. Canepa, P. Traverso, *J. Alloys Compd.* **695** (2017) 2180 (https://doi.org/10.1016/j.jallcom.2016.11.066)
22. H. Ezuber, A. El-Houd, F. El-Shawesh, *Mater. Des.* **29** (2008) 801 (https://doi.org/10.1016/j.matdes.2007.01.021)
23. A. Dobrowska, B. Adamczyk-Cieślak, J. Mizera, K. J. Kurzydłowski, A. Kiełbus, *Arch. Metall. Mater.* **61** (2016) 209 (https://doi.org/10.1515/amm-2016-0038)
24. W. R. Osorio, N. Cheung, L. C. Peixoto, A. Garcia, *Int. J. Electrochem. Sci.* **4** (2009) 820 (www.electrochemsci.org/papers/vol4/4060820.pdf)
25. A. Wiengmoon, P. Sukchot, N. Tareelap, J. T. H. Pearce, T. Chairuangsri, *Arch. Metall. Mater*. **60** (2015) 881 (https://doi.org/10.1515/amm-2015-0223)
26. Y. Wu, H. Liao, *J. Mater. Sci. Technol.* **29** (2013) 380 (https://doi.org/10.1016/j.jmst.2013.02.001)
27. J. R. Davis, *Corrosion of aluminum and aluminum alloys*, ASM International, Materials Park, OH, 1999, pp. 34, 106 (ISBN 978-0-87170-629-4)
28. P. Chen, L. Liang, G. Luo, J. Zeng, *Adv. Mater. Res.* **900** (2014) 96 (https://doi.org/10.4028/www.scientific.net/AMR.900.96)
29. F. Toptan, A. C. Alves, I. Kerti, E. Ariza, L. A. Rocha, *Wear* **306** (2013) 27 (https://doi.org/10.1016/j.wear.2013.06.026)
30. G. Svenningsen, J. E. Lein, A. Bjorgum, J. H. Nordlien, Y. Yu, K. Nisanciogly, *Corros. Sci.* **48** (2006) 226 (https://doi.org/10.1016/j.corsci.2004.11.025)
31. A. S. Sani, I. Aliyu, E. Polycarp, *J. Sci. Eng. Res.* **3** (2012) 1 (https://www.researchgate.net/publication/273946238)
32. S.-L. Lee, Y.-C. Cheng, W.-C. Chen, C.-K. Lee, A.-H. Tan, *Mater. Chem. Phys*. **135** (2012) 503 (https://doi.org/10.1016/j.matchemphys.2012.05.015)
33. J. Campbell, M. Tiryakioğlu, *Mater. Sci. Technol.* **26** (2010) 262 (https://doi.org/10.1179/174328409X425227)
34. Y. Sui, Q. Wang, G. Wang, T. Liu, *J. Alloys Compd.* **622** (2015) 572 (https://doi.org/10.1016/j.jallcom.2014.10.148)
35. C. Liang, Z.-H. Chen, Z.-Y. Huang, F.-Q. Zu, *Mater. Sci. Eng., A* **690** (2017) 387 (https://doi.org/10.1016/j.msea.2017.03.016)
36. C. Bidmeshki, V. Abouei, H. Saghafian, S. G. Shabestari, M. T. Noghani, *J. Mater. Res. Technol.* **5** (2016) 250 (https://doi.org/10.1016/j.jmrt.2015.11.008)
37. Y. S. Jiménez, M. T. Gil, M. T. Guerra, L. S. Baltes, J. C. M. Rosca, *Bull. Transylv. Univ. Braşov Ser. I* **2** (2009) 197 (https://pdfs.semanticscholar.org/13ca/e21c63310a59ab777d1b7411f1d1b9b71319.pdf)
38. S. Mladenovic, *Korozija materijala*, TMF, Blgrade, 1978, p. 112 (In Serbian)
39. S. Gudić, L. Vrsalović, M. Kliškić, I. Jerković, A. Radonić, M. Zekić, *Int. J. Electrochem. Sci.* **11** (2016) 998 (http://www.electrochemsci.org/papers/vol11/110200998.pdf)
40. M. S. Kaiser, M. R. Qadir, S. Dutta, *J. Mech. Eng.* **45** (2015) 48 (https://doi.org/10.3329/jme.v45i1.24384)
41. A. Hossain, F. Gulshan, A. S. W. Kurny, *J. Electrochem. Sci. Eng.* **5** (2015) 173 (https://doi.org/10.5599/jese.174).